Research Article Vol. 29, No. 2 / 18 January 2021 / Optics Express 903
Optics EXPRESS

Predicting lifetime of optical components with Bayesian inference

LINAS SMALAKYS* AND ANDRIUS MELNINKAITIS

Laser Research Center, Vilnius University, Saulėtekio ave. 10, LT- 10223 Vilnius, Lithuania
**linas.smalakys@ff.vu.lt*

Abstract: Virtually all optical materials degrade over time when they are used in high average power or intensity optical systems. Extrapolation of optical components lifetime is crucial in such applications in order to avoid downtime or project failure. Measurements of the laser-induced damage threshold (LIDT) fatigue are usually done using the so-called S-on-1 test described in the ISO 21254-2 standard. The standard, however, suggests only rudimentary techniques for extrapolating LIDT, which are rarely used in practice, therefore, the goal of this work was to provide a framework for analyzing LIDT fatigue data using well established methods of Bayesian statistics. Numerical S-on-1 experiments (assuming constant fatigue) were performed for cases of online detection, interval detection and offline detection. Appropriate lifetime distributions were determined and used to fit simulated data taking into consideration data censoring. Credible intervals of lifetime predictions were determined using Markov chain Monte Carlo (MCMC) technique and compared with results from multiple experiments. The Bayesian lifetime analysis method was compared with technique described in the ISO 21254-2 standard for cases of low and high defect densities. Finally, the outlined extrapolation technique was applied to extrapolate lifetime of HR dielectric mirror.

1. Introduction

Virtually all optical materials degrade over time when they are used in high average or peak power optical systems [1–3]. The decrease of laser-induced damage threshold (LIDT) at longer irradiations as compared to single pulse irradiation is commonly known as the optical fatigue effect. The magnitude of this effect is usually quantified by performing standardized [4,5] S-on-1 tests (S – number of pulses) which measure probabilistic time to failure data at multiple fluence values. Raw data of S-on-1 experiments is usually processed to yield LIDT as a function of number of pulses – the characteristic damage curve (CDC) [4]. The CDC is better known as the stress-life curve [6] outside of laser-induced damage community. Due to budgetary limitations, S-on-1 tests are usually performed up to a relatively small number of pulses (as compared to the design lifetime) therefore extrapolation of measured LIDT is needed in order to predict the lifetime of optical components at application fluences [7].

Experimental and theoretical studies have shown the existence of several fatigue mechanisms in optical components [8], mainly weak statistical fatigue which might arise due to presence of fabrications defects and unstable laser irradiation [9,10] and material modification fatigue due to native and laser-induced states of the material [11–13]. Material modification fatigue usually dominates at longer irradiations [7,8,14], therefore it is the interest of long-term fatigue studies. It was shown that material modification mode can be separated from statistical fatigue mode by performing morphological analysis of every test site either manually or computationally [15]. Unfortunately, further studies determined that the extrapolation model provided in the ISO 21254-2 standard [5] applies only to statistical fatigue, but not material modification fatigue [7].

The ISO 21254 standard also ignores an important topic of censored data [6] in S-on-1 experiments. Data censoring can occur due to failure mode separation, limited irradiation time, sensitivity and speed of online damage detection, use of offline damage detection as well as

#410844 https://doi.org/10.1364/OE.410844
Journal © 2021 Received 23 Sep 2020; revised 2 Dec 2020; accepted 2 Dec 2020; published 5 Jan 2021

Optics EXPRESS

the choice of S-on-1 protocol – all of which contribute to the final uncertainty of extrapolated lifetime prediction.

In this paper, inspired by the advantages Bayesian statistics offers in the analysis of 1-on-1 damage probability data [16], we aim to develop and investigate extrapolation method based on Bayesian inference in order to improve prediction of material modification fatigue observed in S-on-1 experiments.

2. Methods

S-on-1 tests produce probabilistic time to failure (t) data at multiple fluence (F) values. Current analysis techniques [5] expect only exact time to failure data obtained with ideal *in situ* damage detection. However, experimental data is usually censored due to limitations of *in situ* detection or use of *ex situ* detection. Fortunately, both exact and censored data can be analyzed using Bayesian inference by constructing a model that combines a stress-life relationship $t(F)$ (fatigue model) together with lifetime distribution $\phi(t)$ at a single stress (fluence) level (Fig. 1).

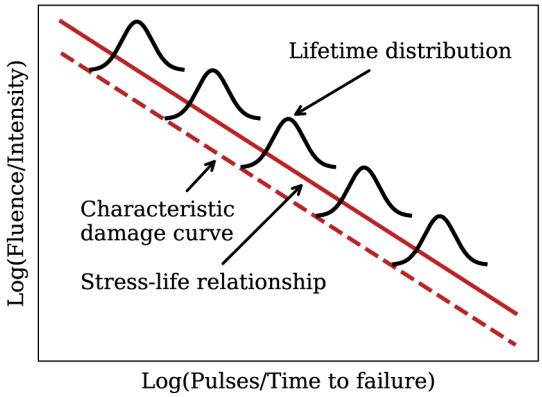

Fig. 1. Schematic representation of how stress-life relationship and lifetime distribution are combined into a single model. This model allows retrieval of characteristic damage curve.

2.1. Stress-life relationship

The stress-life relationship $t(F)$ of material is determined by the physical mechanism of laser-induced damage fatigue. The exact mechanism is rarely known and thus physical models for $t(F)$ are often not available, but the relationship is directly observed in S-on-1 experiments and can hence be approximated based on this data. Throughout this paper we will use the so-called inverse power relationship $t(F) \propto 1/F^{\gamma_1}$ (straight line in log-log stress-life plots) due to its general nature: such relationship was observed above LIDT fatigue limit in both continuous wave [17] and pulsed regimes (ranging from nanosecond [7,9,18] to femtosecond [2,15] pulse durations). The nominal log-life $\mu = \log(t)$ can thus be expressed as a linear function of logarithmic stress $\log(F)$ with parameters γ_0 and γ_1:

$$\mu(F) = \gamma_0 - \gamma_1 \log(F). \tag{1}$$

2.2. Incubation law and simulation of S-on-1 experiments

One of the easiest ways to simulate the incubation process that would result in inverse power relationship (1) is to assume that incubation per laser pulse is constant for every consecutive laser pulse until damage becomes apparent. Assuming non-linear absorption, dose D deposited by a

Optics EXPRESS

single laser pulse at fluence F can be expressed as:

$$D(F) = \left(\frac{F}{F_1}\right)^{\beta}, \tag{2}$$

where β – non-linear absorption factor and F_1 – scaling parameter. Dose D_n deposited by n laser pulses is thus:

$$D_n = \sum_{i=1}^{n} D(F_i). \tag{3}$$

If damage occurs at some critical threshold dose D_T, number of pulses at which damage will occur can be found by solving the inequality $D_n \geq D_T$:

$$D_n = \sum_{i=1}^{n} D(F_i) = \sum_{i=1}^{n} \left(\frac{F_i}{F_1}\right)^{\beta} \geq D_T. \tag{4}$$

Since D_T and F_1 are not independent, we can choose $D_T = 1$ to correspond to single pulse damage at fluence F_1.

A numerical model based on the described incubation mechanism was developed for simulating S-on-1 experiments. A virtual sample was simulated with randomly distributed defects defined by total density d and dose threshold distribution function $g(D_T)$:

$$d = \int_0^{\infty} g(D_T) dD_T. \tag{5}$$

It is important to note, that in the context of material modification fatigue, the word *defects* is used to describe optically active material inhomogeneities and lattice defects [19] instead of fabrication defects. Sample was split into individual non-overlapping test sites and numerically irradiated with a determined number of laser pulses that had Gaussian beam profile:

$$F(x, y; F_0, w_0, x_0, y_0) \propto F_0 \exp\left(-2\frac{(x - x_0)^2 + (y - y_0)^2}{\omega_0^2}\right), \tag{6}$$

where F_0 – peak fluence, $w_0 = d_0/2$ – beam radius at $1/e^2$ intensity level, x_0, y_0 – coordinates of beam center. Local fluence for every defect after every laser pulse was evaluated from the beam profile function (6) and the resulting dose was calculated using (3). Site was considered damaged if any of the defects within that site satisfied damage condition (4) after n pulses.

2.3. Lifetime distributions for degenerate and power-law defects

Even though it was shown that lifetime distributions obtained from S-on-1 experiments can be used to qualitatively distinguish between material modification fatigue and statistical fatigue [8], little work was done to quantitatively describe them. Fortunately, lifetime distributions can be derived for any given defect ensemble and incubation model. Cumulative density function (CDF) of probability that test site will be damaged after pulse (or time) t is equal to probability that at least one defect will be damaged:

$$\Phi_{defects}(t; g, F_0) = 1 - \phi_{Poisson}\left(k = 0; N(t; g, F_0)\right) = 1 - \exp\left(-N(t; g, F_0)\right), \tag{7}$$

where $\phi_{Poisson}$ is probability mass function (PMF) of Poisson distribution, N – average number of defects with dose threshold distribution $g(D_T)$ that can be damaged after t pulses with peak fluence F_0.

Optics EXPRESS

Expression of N for multiple pulses can be derived from a well-known expression of N for a single pulse by substituting threshold fluence with the appropriate incubation model. Given threshold fluence distribution $g(T)$, average number of defects N damaged after a single pulse with peak fluence F_0 is:

$$N(F_0; g) = \int_0^{F_0} g(T)S(T; F_0)\mathrm{d}T, \tag{8}$$

where $S(T; F_0)$ is beam area at fluence T, given peak fluence F_0. For a Gaussian beam:

$$S(T; F_0) = \begin{cases} \frac{\pi\omega_0^2}{2} \ln\left(\frac{F_0}{T}\right), & T \le F_0 \\ 0, & T > F_0 \end{cases}. \tag{9}$$

For the simplest case of degenerate defects (all defects have the same threshold) that are damaged at fluence T_0, the ensemble function $g(T)$ is expressed as:

$$g(T) = \begin{cases} d, & T = T_0 \\ 0, & T \ne T_0 \end{cases}. \tag{10}$$

Assuming incubation model (3) and that all laser pulses are equal, we can rewrite N for multiple pulses with substitution $T = F_1 t^{-1/\beta}$ obtained from (4) with $D_T = 1$:

$$N(t; d, F_0) = \frac{\pi\omega_0^2 d}{2} \ln\left(\frac{F_0}{F_1 t^{-1/\beta}}\right) = N_0 \ln\left(\frac{F_0}{F_1} t^{\frac{1}{\beta}}\right), \tag{11}$$

where $N_0 = \frac{\pi\omega_0^2 d}{2}$. The CDF and probability density function (PDF) of the lifetime distribution for degenerate defects are then respectively:

$$\Phi_{deg}(t; F_0, F_1, N_0, \beta) = \begin{cases} 1 - \left(\frac{F_1}{F_0}\right)^{N_0} t^{-\frac{N_0}{\beta}}, & t \ge t_0 \\ 0, & t < t_0 \end{cases}, \tag{12}$$

$$\phi_{deg}(t; F_0, F_1, N_0, \beta) = \begin{cases} \frac{N_0}{\beta} \left(\frac{F_1}{F_0}\right)^{N_0} t^{-\frac{N_0}{\beta}-1}, & t \ge t_0 \\ 0, & t < t_0 \end{cases}, \tag{13}$$

where $t_0 = \left(\frac{F_1}{F_0}\right)^{\beta}$ is the threshold lifetime at F_0. For large N_0 (high density defects and/or large beams) we get deterministic case:

$$\lim_{N_0 \to \infty} \phi_{deg}(t) = \delta\left(t - \left(\frac{F_1}{F_0}\right)^{\beta}\right). \tag{14}$$

In practice, the observed defect ensembles are rarely degenerate and usually resemble power-law behaviour [20]. A good alternative for practical applications is a log-normal lifetime distribution, which is observed for many types of fatigue data [6]. The CDF of a log-normal distribution expressed using log-location and log-scale parameters (μ and σ respectively) [21] is:

$$\Phi_{log-norm}(t; \mu, \sigma) = \Phi_{norm}\left(\frac{\log(t) - \mu}{\sigma}\right) = \frac{1}{2}\left(1 + \mathrm{erf}\left(\frac{\left(\frac{\log(t)-\mu}{\sigma}\right)}{\sqrt{2}}\right)\right), \tag{15}$$

Optics EXPRESS

while the PDF is:

$$\phi_{log-norm}(t;\mu,\sigma) = \frac{1}{\sigma t}\phi_{norm}\left(\frac{\log(t)-\mu}{\sigma}\right) = \frac{1}{\sigma t}\frac{1}{\sqrt{2\pi}}\exp\left(-\frac{\left(\frac{\log(t)-\mu}{\sigma}\right)^2}{2}\right), \tag{16}$$

where Φ_{norm} and ϕ_{norm} are respectively CDF and PDF of the standard normal distribution, erf – the error function. The log-location parameter μ is retrieved from the stress-life relationship, e.g. the inverse power relationship (1). The log-scale parameter σ can either be assumed to be constant, or it can also be modeled as a function of stress F if needed. Since the log-normal distribution is a continuous function, the threshold lifetime is evaluated as some percentile of the distribution, with 1st and 5th percentiles (corresponding to 1% and 5% damage probability) being the most common [6]. In the context of this paper, 1st percentile was used as the threshold lifetime.

In order to compare lifetime distributions of samples with degenerate and power-law defects, irradiation of 1000 test sites at single fluence value was simulated (Fig. 2). It can be seen that the derived lifetime distribution for degenerate defects (13) correctly reproduces the experimental results (Fig. 2(b)), while the log-normal distribution (16) is a good approximation for lifetime distribution of power-law defects (Fig. 2(d)).

2.4. Maximum a posteriori probability for S-on-1 experiments

Bayesian statistics gives a framework for evaluating posterior probability of the model $\Phi(\theta)$ given observed time to failure data Δ [22]:

$$P(\Phi|\Delta) = \frac{P(\Delta|\Phi)P(\Phi)}{P(\Delta)}, \tag{17}$$

where $P(\Delta|\Phi)$ – likelihood of the data Δ given the model Φ, $P(\Phi)$ – prior probability of the model Φ (beliefs about the model Φ before data is taken into account), $P(\Delta)$ – probability of data Δ. Since $P(\Delta)$ depends only on data and is difficult to evaluate in practice, usually only the product of likelihood function and prior probability is considered:

$$P(\Phi|\Delta) \propto P(\Delta|\Phi)P(\Phi). \tag{18}$$

Log-posterior is more often used in practical applications to maintain numerical accuracy [22]:

$$\log P(\Phi|\Delta) \propto \log P(\Delta|\Phi) + \log P(\Phi). \tag{19}$$

The best fit of model's parameters θ_{fit} is evaluated by performing maximum a posteriori probability (MAP) estimation: analytically or numerically maximizing the log-posterior $\log P(\Phi|\Delta)$ in respect to model's parameters.

As mentioned in the introduction, data reduction techniques to obtain damage probability from S-on-1 experiments ignore data censoring. In contrast, constructing likelihood function for the lifetime observations allows accurate interpretation of both censored and complete data [6]. Likelihood $\mathcal{L}_i$ of a single test site i is evaluated from the lifetime distribution (Fig. 3):

$$\mathcal{L}_i = \begin{cases} \phi(t_i), & \text{exact: damage occurred at } t_i \\ \Phi(t_i), & \text{left-censored: damage occurred in interval } (0, t_i) \\ \Phi(t_i) - \Phi(t_{i-1}), & \text{interval-censored: damage occurred in interval } (t_{i-1}, t_i) \\ 1 - \Phi(t_i), & \text{right-censored: damage will occur in interval } (t_i, \infty) \end{cases}. \tag{20}$$

Optics EXPRESS

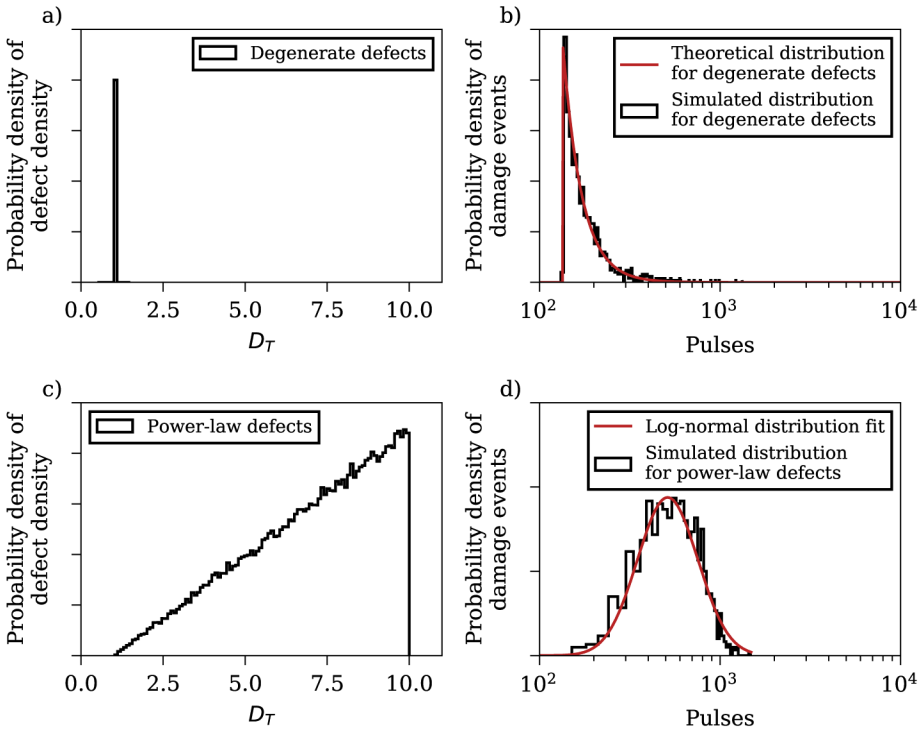

Fig. 2. Comparison of dose threshold distributions for degenerate (a) and power-law (c) defects and their corresponding lifetime distributions (b, d) (all vertical scales are linear). Irradiation of 1000 test sites was simulated with peak fluence of 3 J/cm^2 and beam diameter of 200 µm. Incubation model was simulated with $F_1 = 8$ J/cm^2, $\beta = 5$. Degenerate defect ensemble (a) was simulated with parameters $D_T = 1$, $d = 10^5$ cm^{-2} while the linear power law distribution (c) with parameters $D_{T,min} = 1$, $D_{T,max} = 10$, $d = 5 \cdot 10^5$ cm^{-2}. Red line in (b) corresponds to derived theoretical lifetime distribution of degenerate defects (13), while red line in (d) corresponds to approximation of lifetime distribution with log-normal function (16).

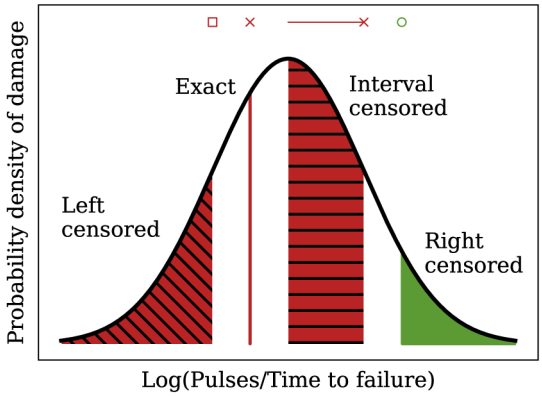

Fig. 3. Comparison of exact and censored observations given PDF of log-normal lifetime distribution. Exact measurement, as well as left-censored and interval-censored measurements correspond to damaged test sites, while right-censored measurements correspond to non-damaged sites. Markers at the top of the graph represent how censored data is represented in stress-life plots.

Optics EXPRESS

Exact observations are usually obtained with online damage detection methods (such as back-scattered light detection with photodiodes) in pulsed regime, where it is possible to determine the exact pulse after which damage has occurred:

$$\mathcal{L}_i^{(exact)} = \phi(t_i). \tag{21}$$

Interval-censored observations are obtained for all continuous wave (CW) lasers and for pulsed lasers when damage detection rate is slower than pulse repetition rate. In this case the damage has occurred between pulses (or times) t_i and t_{i-1}, therefore the corresponding likelihood is:

$$\mathcal{L}_i^{(interval)} = \int_{t_{i-1}}^{t_i} \phi(t)\mathrm{d}t = \Phi(t_i) - \Phi(t_{i-1}). \tag{22}$$

Left-censoring occurs when damage is detected at the first observation, i.e. all that is known is that damage has occurred at time interval $(0, t_i)$. This type of censored data is common in practice, because more sensitive offline damage detection (e.g. Nomarski or atomic force microscopy) is often performed after the experiment. The likelihood for left-censored data is thus:

$$\mathcal{L}_i^{(left)} = \int_{0}^{t_i} \phi(t)\mathrm{d}t = \Phi(t_i) - \Phi(0) = \Phi(t_i). \tag{23}$$

Right-censoring occurs when irradiation is stopped before damage is reached or when damaged sites are determined to belong to the failure mode other than the one analysed. Failure will occur in the interval (t_i, ∞) therefore the likelihood for right-censored data can be expressed as:

$$\mathcal{L}_i^{(right)} = \int_{t_i}^{\infty} \phi(t)\mathrm{d}t = \Phi(\infty) - \Phi(t_i) = 1 - \Phi(t_i). \tag{24}$$

Single LIDT test can contain any combination of exact and left-, right- or interval-censored observations. The total likelihood of the S-on-1 test with N test sites is obtained by multiplying likelihoods of individual test sites [6]:

$$\mathcal{L} = \prod_{i=1}^{N} \mathcal{L}_i. \tag{25}$$

The total log-likelihood for all test sites, assuming inverse power relationship (1) and log-normal lifetime distribution (16), is thus a three parameter $(\gamma_0, \gamma_1, \sigma)$ function:

$$\log P(\Delta|\Phi) \equiv \log \mathcal{L} = \sum_{i=1}^{N} \log \mathcal{L}_i(t_i; \mu(F_i; \gamma_0, \gamma_1), \sigma). \tag{26}$$

The log-prior probability distribution $\log P(\Phi)$ in (19) is constructed by including any additional information known about the model's parameters (e.g. upper limit of LIDT from previous experiments). Constructing informative and non-informative priors [22] is outside the scope of this paper, therefore only simple flat priors were used within the allowed values of models' parameters: $\sigma \in (0, \infty)$, $\gamma_0 \in (-\infty, \infty)$, $\gamma_1 \in (0, \infty)$. Using full posterior probability (19) instead of just likelihood function (26) (as in maximum likelihood estimation – MLE) allows use of probability distribution sampling algorithms for uncertainty estimation.

2.5. Optimization and uncertainty evaluation

In this work, MAP estimation of the log-posterior function (19) was performed with open-source implementation of the sequential least squares programming (SLSQP) optimization method [23].

Optics EXPRESS

The uncertainty of estimated parameters was evaluated with Markov chain Monte Carlo (MCMC) technique which draws samples from the continuous posterior probability distribution (19) with probability density of those samples proportional to the analytical distribution. Once the samples are drawn, they can be marginalized to evaluate the uncertainty of model's parameters or projected into stress-life space to evaluate lifetime uncertainty by constructing highest posterior density (HPD) intervals [22]. Even though MCMC methods are easy to interpret, they are computationally intensive. Fortunately, the recent development of freely accessible implementations of MCMC algorithms allows practitioners to easily apply this powerful technique in practice. In this work, an open-source implementation [24] of affine invariant MCMC sampler [25] was used to perform the sampling. A total of 200 virtual walkers were used to perform the random walk procedure for 100 steps in order to sample the distribution (using 50 last steps in further analysis to avoid non-converged data). On a typical desktop computer MAP estimation is performed in a few seconds, while MCMC sampling for uncertainty evaluation takes several minutes to complete (the duration is highly dependent on the number of virtual walkers and steps).

3. Results and discussion

3.1. Investigation of S-on-1 protocols with simulated data

S-on-1 simulations were performed for up to 10^4 laser pulses at fluence levels exponentially spaced between 1 and 10 J/cm^2 with 25 test sites per fluence level (as recommended by the ISO 21254-2 standard). Gaussian beam with 200 μm beam diameter at 1/e^2 level with 5% energy and diameter instability was used for irradiation. Previously described incubation law (4) with parameters $F_1 = 8$ J/cm^2, $\beta = 5$ was used to simulate cases of both low density (10^4 cm^{-2}) and high density ($5 \cdot 10^5$ cm^{-2}) defects. Linear power-law distribution ($D_{T,min} = 1$, $D_{T,max} = 10$) was used for the defect ensemble (the same distribution as in Fig. 2(c)). Three S-on-1 protocols differing in their damage detection mechanisms were chosen for investigation of Bayesian lifetime analysis:

1. Exact online detection protocol - damage detection is performed at the same rate as the pulse repetition rate and irradiation is immediately stopped in case of damage. This is the most common S-on-1 protocol outlined in the ISO 21254-2 standard which produces exact observations of damage events.

2. Interval online detection protocol - damage detection is performed at the rate slower than the pulse repetition rate and irradiation is immediately stopped in case of damage. Specifically, damage detection after 1, 10, 100, 1000 and 10000 laser pulses was used. This protocol produces interval-censored observations of damage events, i.e. if damage was detected after 1000 pulses, we know that it occurred between 100 and 1000 pulses.

3. Offline detection protocol - damage detection is performed after the test. This requires selecting values for fluence and number of pulses that form a grid on stress-life plot and irradiating test sites independently of the state of damage. This S-on-1 protocol is also outlined in the ISO 21254-2 standard as an alternate method when online damage detection is not available. This protocol produces left-censored observations of damage as well as substantially more right-censored observations compared to the other protocols.

Simulated data was extrapolated using both the approach outlined in the ISO 21254-2 standard as well as Bayesian lifetime analysis using MAP estimation. The standard approach is a two step process: first, the experimental CDC curve is determined by performing linear regression on damage probability at selected pulse classes (25 for exact online and offline detection protocols, 5 for interval online detection protocol); second, the experimental CDC curve is fitted with extrapolation curve (all optimization steps are performed using least squares approach). The MAP

Optics EXPRESS

estimation approach requires just a single optimization step to maximize posterior probability (19). Additional MCMC run was performed to evaluate uncertainty of the MAP estimation. Inverse power relationship between peak fluence and number of pulses (1) was used as the extrapolation curve in both cases.

Single simulations for each combination of defect density and S-on-1 protocol are provided in Fig. 4. We see that the MAP estimation analysis produced results that are closer to true LIDT values than the standard approach for all simulated cases. The accuracy of standard approach suffers at lower defect density, especially for offline damage detection protocol case (Fig. 4(c)). This is mainly caused by the fact that data-reduction technique for damage probability outlined in the ISO 21254-2 standard is not suitable for left-censored data. Also, large percentage of right-censored data reduced the accuracy of this test (as seen in wider credible region obtained with MCMC for MAP estimate).

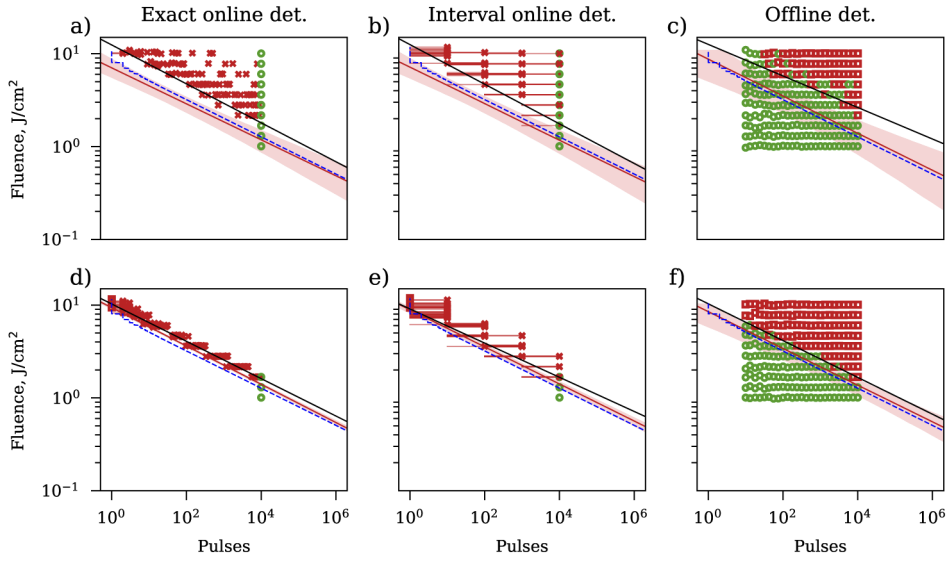

Fig. 4. Comparison of simulated S-on-1 experiments for low density (10^4 cm^{-2}) (a-c) and high density ($5 \cdot 10^5$ cm^{-2}) power-law defects (d-f). Simulations were performed for 200 µm beam diameter ($1/e^2$) and 5% energy and diameter instability. Blue dashed line represents true LIDT from fatigue model, black solid line – ISO extrapolation, red solid line – Bayesian lifetime extrapolation (1st percentile), light red area – 95% credible HPD region for Bayesian lifetime extrapolation retrieved from MCMC sampling.

Accuracy and repeatability of extrapolation approaches was compared by performing 100 simulations for each combination of defect density and S-on-1 protocol. LIDT values extrapolated to 10^6 laser pulses are provided in Fig. 5. We see that MAP estimation analysis produced both more precise and repeatable LIDT values for all tested cases. Interestingly, accuracy and repeatability of exact online and interval online detection protocols was very similar. Offline detection protocol produced wider spread of LIDT values as predicted by MCMC credible regions in Fig. 4.

The standard approach appears to be more sensitive to discretization of fluence levels than MAP estimation, because it produced multimodal LIDT distribution for the case of interval online detection protocol with high density defects (white distribution in middle column of Fig. 5(b)). This effect may be caused by the fact that the standard approach is based on measuring damage probability instead of the directly observed lifetime data which is used by the MAP estimation.

Optics EXPRESS

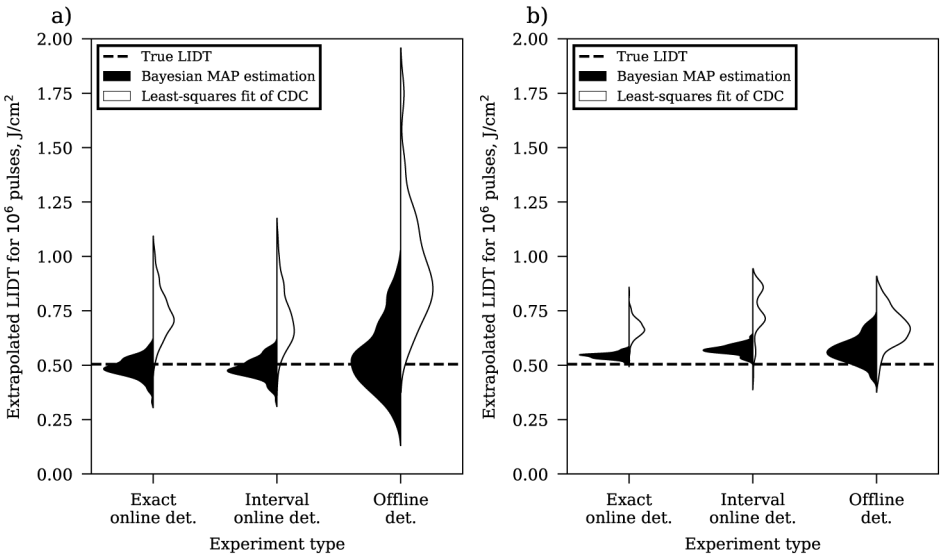

Fig. 5. Comparison of LIDT extrapolation to 10^6 pulses (from experiments performed up to 10^4 pulses) for low density (10^4 cm^{-2}) defects (a) and high density ($5 \cdot 10^5$ cm^{-2}) defects (b). Each violin plot represents 100 experiments analyzed using Bayesian lifetime analysis and standard ISO extrapolation.

3.2. *Predicting lifetime of HR dielectric mirror*

The developed Bayesian lifetime analysis based on MAP estimation was applied to experimental interval-censored S-on-1 data [7] for highly-reflective (HR) dielectric mirror. The sample was coated using ion beam sputtering (IBS) on a conventionally polished 25.4 mm diameter fused silica substrate. The S-on-1 experiment was performed at a wavelength of 355 nm, pulse duration of 10 ns, repetition rate of 100 Hz, beam diameter of 209 μm and angle of incidence of 45 deg. The test bench included both a photodiode and a differential interference contrast (DIC) microscope for online damage detection. The photodiode was used for measuring back-scattered light and offered fast damage detection after every laser pulse, while online DIC microscope was used to separate damage caused fabrication defects from damage caused by material modification. DIC microscopy images were collected after pulses 1, 2, 3,. . . , 10, 20, 30,. . . , 10^7. More experimental details are provided in Ref. [7].

Test results for material modification failure mode are provided in Fig. 6(a). Right-censoring of test sites up to around 10^3 laser pulses was caused by online back-scattered light detection due to defect-driven damage, while right-censoring of test sites after 10^3 laser pulses was due to limited number of pulses allowed for irradiation. All of the damaged test-sites were interval-censored due to semi-online nature of DIC microscopy damage detection. MAP estimation was performed on posterior probability function (19) assuming inverse power stress-life relationship (1) and log-normal lifetime distribution (16). MCMC run was performed to evaluate uncertainty of the estimate (Fig. 7). The lifetime of HR coating was estimated for applications at 1 J/cm^2 and 0.5 J/cm^2 and resulted in most likely values of 2.9 and 34.0 million laser pulses respectively with 95% credible HPD intervals of 0.1–10.5 and 0.7–175.7 million laser pulses (Fig. 6(b)).

It is important to note, that the single test site at 10^7 laser pulses (the so-called validation point) was included in the MAP estimation. Evaluating damage probability at 10^7 laser pulses and including such point into the extrapolation approach outlined in ISO 21254-2 would be impossible due to lack of non-damaged test sites at/above 10^7 pulses.

Optics EXPRESS

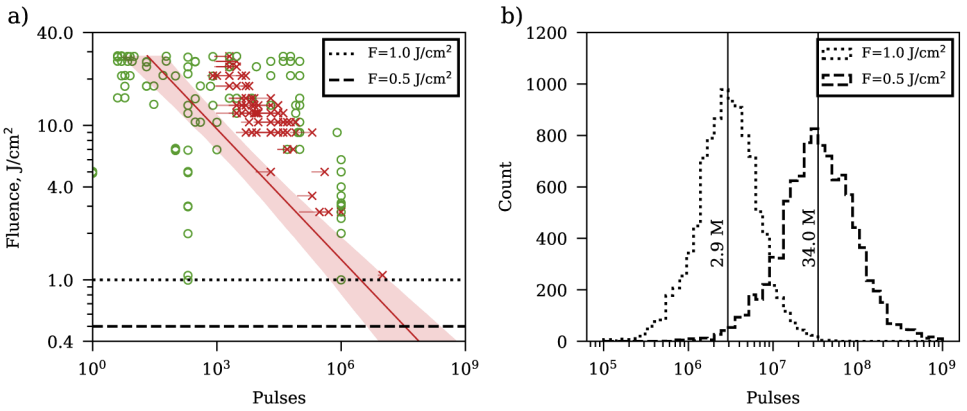

Fig. 6. Fit of experimental data (a) and lifetime prediction at two application fluences (b). Red line corresponds to Bayesian MAP estimation while surrounding red area corresponds to 95 % credible interval obtained with MCMC. The lifetime was estimated for applications at 1 J/cm^2 (median value of 2.9 million laser pulses with 95% credible HPD interval of 0.1–10.5 million laser pulses) and 0.5 J/cm^2 (median value of 34.0 million laser pulses with 95% credible HPD interval of 0.7–175.7 million laser pulses).

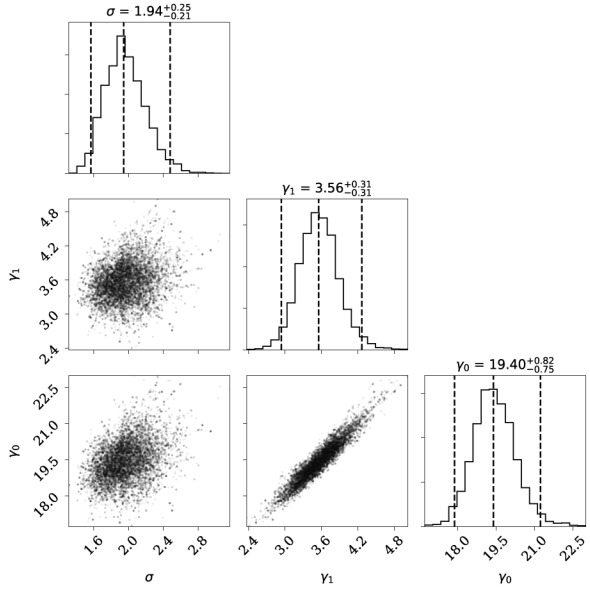

Fig. 7. Corner plot of MCMC samples which correspond to credible interval in Fig. 6. Parameter σ corresponds to log-scale of log-normal lifetime distribution (16) while γ_0 and γ_1 are parameters of inverse power stress-life relationship (1). Dashed vertical lines represent 95% credible HPD intervals.

Optics EXPRESS

4. Conclusions

In conclusion, we have developed the Bayesian lifetime analysis approach based on MAP estimation for the analysis of S-on-1 laser-induced damage fatigue experiments. Lifetime distribution for the simplest case of degenerate defect ensemble was derived and statistical log-normal distribution was suggested as an approximation for lifetime distribution of power-law defects. MAP estimation produced more accurate and repeatable extrapolation results as compared to the standard extrapolation approach for all simulated S-on-1 protocols due to correct treatment of censored observations. Credible HPD intervals retrieved from single S-on-1 experiment using MAP estimation correlated with uncertainties resulting from both the S-on-1 test protocol (different damage detection mechanisms) as well as the statistical nature of damage (different defect densities).

Lifetime prediction of material modification mode for HR dielectric coating was performed at two application fluence values using interval-censored experimental S-on-1 results that could not be interpreted with standard approach. The lifetime was estimated for applications at 1 J/cm^2 (median value of 2.9 million laser pulses with 95% credible HPD interval of 0.1–10.5 million laser pulses) and 0.5 J/cm^2 (median value of 34.0 million laser pulses with 95% credible HPD interval of 0.7–175.7 million laser pulses).

Funding. European Regional Development Fund (01.2.2-LMT-K-718-01-0014).

Acknowledgments. The authors would like to thank Lidaris Ltd. for providing unique interval-censored raw experimental test data to perform the lifetime analysis (under the cooperation agreement BS-120000-1018).

Disclosures. The authors declare that there are no conflicts of interest related to this article.

References

1. A. E. Chmel, "Fatigue laser-induced damage in transparent materials," Mater. Sci. Eng., B **49**(3), 175–190 (1997).
2. M. Ďurák, P. K. Velpula, D. Kramer, J. Cupal, T. Medrík, J. Hrebícek, J. Golasowski, D. Peceli, M. Kozlová, and B. Rus, "Laser-induced damage threshold tests of ultrafast multilayer dielectric coatings in various environmental conditions relevant for operation of ELI beamlines laser systems," Opt. Eng. **56**(1), 011024 (2016).
3. C. Danson, D. Hillier, N. Hopps, and D. Neely, "Petawatt class lasers worldwide," High Power Laser Sci. Eng. **3**, e3 (2015).
4. "ISO 21254-1:2011 Lasers and laser-related equipment – Test methods for laser-induced damage threshold – Part 1: Definitions and general principles," Standard, International Organization for Standardization, Geneva, Switzerland (2011).
5. "ISO 21254-2:2011 Lasers and laser-related equipment – Test methods for laser-induced damage threshold – Part 2: Threshold determination," Standard, International Organization for Standardization, Geneva, Switzerland (2011).
6. W. B. Nelson, *Accelerated Testing: Statistical Models, Test Plans, and Data Analysis* (Springer, 2004).
7. A. Melninkaitis, G. Batavičiutė, C. Heese, M. Ščiuka, and L. Smalakys, "Towards qualification longevity of high power Space optics," Proc. SPIE **11180**, 1118085 (2019).
8. F. Wagner, A. Beaudier, and J.-Y. Natoli, "Discussing defects related to nanosecond fatigue laser damage: a short review," Opt. Eng. **57**(12), 1 (2018).
9. C. Gouldieff, F. Wagner, and J.-Y. Natoli, "Nanosecond uv laser-induced fatigue effects in the bulk of synthetic fused silica: a multi-parameter study," Opt. Express **23**(3), 2962–2972 (2015).
10. A. Melninkaitis, J. Mirauskas, M. Jupé, D. Ristau, J. W. Arenberg, and V. Sirutkaitis, "The effect of pseudo-accumulation in the measurement of fatigue laser-induced damage threshold," Proc. SPIE **7132**, 713203 (2008).
11. A. Beaudier, F. R. Wagner, and J. Y. Natoli, "Using NBOHC fluorescence to predict multi-pulse laser-induced damage in fused silica," Opt. Commun. **402**, 535–539 (2017).
12. L. A. Emmert, M. Mero, and W. Rudolph, "Modeling the effect of native and laser-induced states on the dielectric breakdown of wide band gap optical materials by multiple subpicosecond laser pulses," J. Appl. Phys. **108**(4), 043523 (2010).
13. L. Smalakys, B. Momgaudis, R. Grigutis, S. Kičas, and A. Melninkaitis, "Contrasted fatigue behavior of laser-induced damage mechanisms in single layer ZrO2 optical coating," Opt. Express **27**(18), 26088–26101 (2019).
14. F. R. Wagner, C. Gouldieff, J. Y. Natoli, and M. Commandré, "Nanosecond multi-pulse laser-induced damage mechanisms in pure and mixed oxide thin films," Thin Solid Films **592**, 225–231 (2015).
15. L. Smalakys, E. Švažas, R. Grigutis, and A. Melninkaitis, "Application of image processing and machine learning for classification of laser-induced damage morphology," Proc. SPIE **10805**, 108052B (2018).
16. G. Batavičiutė, P. Grigas, L. Smalakys, and A. Melninkaitis, "Revision of laser-induced damage threshold evaluation from damage probability data," Rev. Sci. Instrum. **84**(4), 045108 (2013).

Optics EXPRESS

17. K. Slinker, J. Pitz, S. Sihn, and J. P. Vernon, "Determining and scaling continuous-wave, laser-induced damage thresholds of thin reflectors," Opt. Express **27**(4), 4748–4757 (2019).
18. F. R. Wagner, C. Gouldieff, and J.-Y. Natoli, "Contrasted material responses to nanosecond multiple-pulse laser damage: from statistical behavior to material modification," Opt. Lett. **38**(11), 1869–1871 (2013).
19. A. Melninkaitis, N. Šiaulys, L. Smalakys, B. Momgaudis, J. Vaicenavičius, S. Barkauskaitė, V. Sirutkaitis, L. Gallais, and S. Guizard, "What time-resolved measurements tell us about femtosecond laser damage?" Proc. SPIE **9632**, 96320O (2015).
20. G. Batavičiutė, M. Ščiuka, and A. Melninkaitis, "Direct comparison of defect ensembles extracted from damage probability and raster scan measurements," J. Appl. Phys. **118**(10), 105306 (2015).
21. F. Pascual, W. Meeker, and L. Escobar, "Accelerated life test models and data analysis," in *Springer Handbook of Engineering Statistics*, H. Pham, ed. (Springer, 2006).
22. A. Gelman, J. B. Carlin, H. S. Stern, D. B. Dunson, A. Vehtari, and D. B. Rubin, *Bayesian Data Analysis* (CRC, 2014), 3rd ed.
23. P. Virtanen, R. Gommers, T. E. Oliphant, M. Haberland, T. Reddy, D. Cournapeau, E. Burovski, P. Peterson, W. Weckesser, J. Bright, S. J. van der Walt, M. Brett, J. Wilson, K. J. Millman, N. Mayorov, A. R. J. Nelson, E. Jones, R. Kern, E. Larson, C. J. Carey, İ. Polat, Y. Feng, E. W. Moore, J. VanderPlas, D. Laxalde, J. Perktold, R. Cimrman, I. Henriksen, E. A. Quintero, C. R. Harris, A. M. Archibald, A. H. Ribeiro, F. Pedregosa, and P. van Mulbregt, and SciPy 1.0 Contributors, "SciPy 1.0: Fundamental Algorithms for Scientific Computing in Python," Nat. Methods **17**(3), 261–272 (2020).
24. D. Foreman-Mackey, D. W. Hogg, D. Lang, and J. Goodman, "emcee: The MCMC hammer," Publ. Astron. Soc. Pac. **125**(925), 306–312 (2013).
25. J. Goodman and J. Weare, "Ensemble samplers with affine invariance," Commun. Appl. Math. Comput. Sci. **5**(1), 65–80 (2010).